Evaluating the Meteorological Pattern of District Swat Using Different SSP Scenarios

Fayaz Ahmad Khan[1], Hamid Hussain[2], Saqib Mahmood[3], Afed Ullah Khan[3]
[1]National institute of urban infrastructure planning, University of Engineering and Technology, Peshawar, 2500, Pakistan
[2]Department of Civil Engineering, University of Engineering and Technology Mardan, Mardan 23200, Pakistan
[3]Department of Civil Engineering, Campus III-Bannu, University of Engineering and Technology Peshawar, Bannu 28100, Pakistan
*__Correspondence__: afedullah@uetpeshawar.edu.pk

Citation | Khan. F. A, Hussain. H, Mahmood. S, Khan. A. U, "Evaluating Meteorological Patterns of District Swat Using Different SSP Scenario", IJIST, Vol. 07, Issue. 03 pp 1739-1753, Aug 2025
DOI | https://doi.org/10.33411/ijist/20257317391753
Received | June 18, 2025 **Revised |** July 30, 2025 **Accepted |** Aug 01, 2025 **Published |** Aug 02, 2025.

This study investigates the observed and projected impacts of climate change in District Swat, Pakistan, using meteorological records and CMIP6-based projections under SSP2-4.5 and SSP5-8.5 scenarios. Metrological variables, such as temperature and precipitation, were examined for long-term trends, anomalies, and extremes. Machine learning techniques (XGBoost and SHAP) were used to identify the most relevant online datasets and climate models. ERA5 emerged as the most reliable online source, and INM-CM5-0, CNRM-CM6-1, and CMCC-ESM2 were selected as the best-performing GCMs. The Mann-Kendall test showed a significant rise in minimum and maximum temperatures based on future conditions. For instance, the maximum temperature under SSP5-8.5 had a significant increasing trend with a Kendall Tau value of 0.1517, a Sen Slope of 0.00018, and a p-value less than 0.001. In the meantime, the trend of precipitation under SSP2-4.5 was decreasing significantly, which indicated the likelihood of an even more arid future. Under SSP5-8.5, temperature anomalies might be as high as 6.5°C, and precipitation anomalies could be as low as -1.5 mm or as high as +2 mm. Furthermore, Intensity-Duration-Frequency (IDF) analysis indicated that extreme rainfall events are projected to intensify, with rainfall intensities for the 100-year return period increasing from an observed value of 340 mm/hr to 360 mm/hr under SSP5-8.5. These outcomes show a potential rising trend of warmer and possibly drier conditions in the Swat District, and higher vulnerability to severe weather conditions. The results show that we need infrastructure that can handle climate change, flexible water management plans, and aggressive planning to lessen the effects of future extreme weather events.

Keywords: Climate Change, GCM, Anomalies, SSPs, IDF, Machine Learning

Introduction:

Climate change is one of the most pressing global issues, exerting profound impacts on both natural ecosystems and human societies [1]. Over recent decades, extensive scientific evidence has pointed to a consistent rise in global and regional temperatures, with this trend expected to continue through the 21st century [2]. According to projections based on climate model simulations, average global temperatures by the end of the century could rise between 1.1°C to 5.4°C (2°F to 9.7°F) above current levels [3]. This shift is already triggering significant changes in hydrological systems, especially in sensitive regions like South Asia, where climate-driven disruptions in rainfall and runoff patterns are becoming increasingly evident [4][5]. One of the most severe manifestations of these disruptions is the alteration of precipitation patterns, leading to increased frequency and intensity of river flows and flood events. Flooding, often surpassing historical boundaries, has become one of the most destructive hydro-meteorological disasters globally. These floods not only result in massive economic losses and infrastructure damage but also threaten human lives, particularly in regions with inadequate prediction and control systems [6]. In 2020 alone, over 33 million people were affected by floods, with 6,171 recorded fatalities, according to the Centre for Research on the Epidemiology of Disasters (CRED, 2021) [7]. Furthermore, between 2008 and 2018, natural disasters displaced around 26.4 million people globally. South Asia accounted for 26.14% of these displacements, underscoring the region's acute vulnerability to climate extremes [6].

Pakistan's geographical diversity plays a central role in its climate sensitivity. The country lies adjacent to the warm Arabian Sea in the south and hosts three major mountain ranges the Himalayas, the Hindu Kush, and the Karakoram along its northern and western boundaries. These mountains contain vast reserves of glacial ice and snow, which are critical to the country's freshwater supply. However, this unique topography also exposes Pakistan to heightened climate risks, especially when coupled with rapid urbanization, deforestation, and other anthropogenic pressures. Since 1998, Pakistan has experienced over 150 extreme weather events, including 14 major floods since 1990, making it one of the most climate-vulnerable countries in the world [8].

Within Pakistan, climatic conditions vary significantly across regions. Northern areas such as Gilgit-Baltistan, Azad Jammu and Kashmir, and upper districts of Khyber Pakhtunkhwa are characterized by cooler temperatures and high precipitation, and serve as vital snowmelt and glacial zones. These regions are critical for sustaining river flow during dry seasons. In contrast, Central Punjab and Upper Sindh exhibit moderate rainfall and temperature levels and are heavily dependent on agriculture. Their agricultural productivity is highly sensitive to climatic variations. Southern Sindh and the southwestern/western regions of Balochistan, on the other hand, suffer from low rainfall and high temperatures, making them chronically drought-prone and water-scarce. This distinct climatic gradient underscores the urgent need for region-specific adaptation strategies in water management and agricultural planning.

Swat District, situated in northern Pakistan within Khyber Pakhtunkhwa, exemplifies a region increasingly threatened by climate-induced flooding. Its mountainous terrain and proximity to snow-fed rivers make it particularly susceptible to intense rainfall and flash floods. The 2010 flood event serves as a stark example: 86 lives were lost, nearly 9,800 livestock perished, and over 40,000 houses were destroyed [9]. Vulnerability calls for continuous monitoring and detailed analysis of flood events to understand how local watersheds respond to sudden precipitation and temperature anomalies [10].

Objectives:

This study aims to analyze the historical and projected climatic trends of District Swat by examining key meteorological parameters, temperature (minimum and maximum), and precipitation, using observed data and CMIP6-based projections under SSP2-4.5 and SSP5-

8.5 scenarios. The research integrates advanced machine learning techniques (XGBoost and SHAP) to identify the most reliable online climate datasets and GCMs specific to the region, enhancing model transparency and accuracy. By applying the Mann-Kendall trend test and developing future Intensity-Duration-Frequency (IDF) curves, the study assesses long-term shifts and extreme rainfall behavior, which are crucial for regional climate resilience.

Novelty Statement:

The novelty of this work lies in its data-driven approach to model selection, high-resolution analysis of a flood-prone mountainous district, and the projection of future climate extremes to inform adaptive infrastructure and water resource planning in a region that has been historically underrepresented in detailed climate impact assessments.

Methodology:

Study Area:

District Swat is a riverine valley located in the Khyber Pakhtunkhwa province of Pakistan, positioned approximately between 35.2° to 35.9° North latitude and 72.0° to 72.8° East longitude. The region receives an average annual precipitation ranging between 700- and 800-mm. Summers, extending from June to September, are marked by heavy rainfall, while winters, from December to February, are notably cold. During summer, average temperatures range from 20°C to 30°C, whereas in winter, they drop to between 0°C and 10°C.

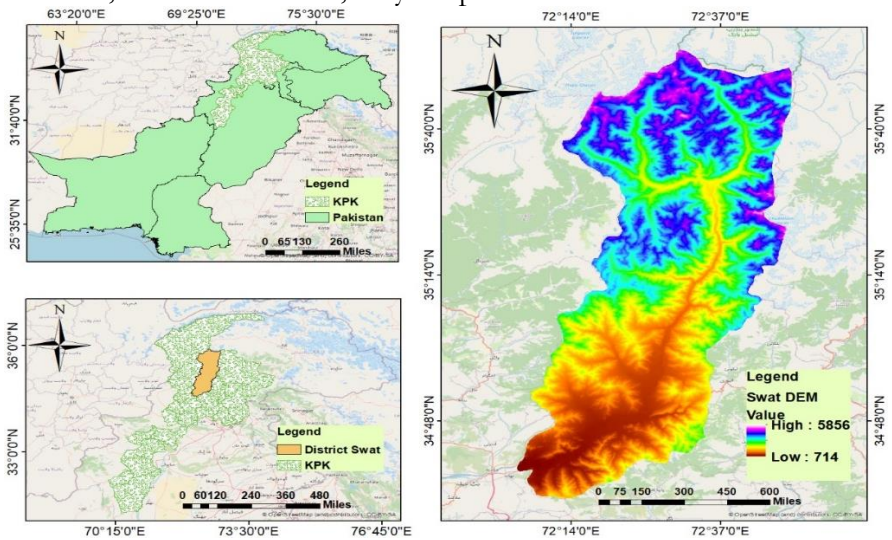

Figure 1. Study Area

Data Collection:

Pakistan faces significant challenges related to data availability, as limited access to reliable and comprehensive data remains a major constraint in various sectors. The data concerning precipitation and mean temperature were taken from the Pakistan Meteorological Department. The data of temperature maximum and temperature minimum was obtained at Climate Forecast System CFS, Climate Hazards Group Infrared Precipitation with Station data (CHIRPS), Climate Prediction Center Unified Precipitation Project (CPC UPP), ERA5-Land data tailored to agricultural purposes (ERA5 Ag), Modern-Era Retrospective analysis for Research and Applications, Version 2 (MERRA-2), National Aeronautics and Space Administration Prediction of Worldwide Energy Resources (NASA POWER), and Precipitation Estimation from Remotely Sensed Information. Additionally, daily climatological data for maximum temperature, minimum temperature, and precipitation were obtained from ten Global Climate Models (GCMs): INM-CM4-8 (Russia), INM-CM5-0 (Russia), NESM3 (China), EC-Earth3-Veg-LR (Europe), GFDL-ESM4 (United States), CMCC-ESM2 (Italy), CNRM-CM6-1 (France), CNRM-ESM2-1 (France), MIROC6 (Japan), and MRI-ESM2-0 (Japan). In the case of precipitation and temperature, data from the most

relevant online resource were displayed using the XGBoost method. Likewise, the most relevant GCMs were also depicted through the XGBoost method. The Shared Socioeconomic Pathways SSP5-8.5 and SSP2-4.5 were used in the analysis, representing high- and moderate-emission scenarios, respectively. Figure 2 shows the overall methodology: first, climatic data were downscaled and bias-corrected; second, precipitation and temperature pattern analysis was conducted using statistical trend detection methods, including the Mann–Kendall (MK) test and Sen's slope estimator; third, drought index and heat wave characteristics were evaluated under both historical and projected climate conditions.

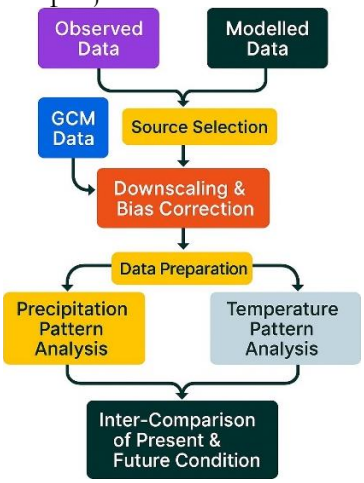

Figure 2. Methodology

Selection of Online Data Sources and GCM Models:

In this study, the Extreme Gradient Boosting (XGBoost) model was applied to rank the importance of various input features in predicting precipitation and temperature over the Swat region. For online dataset selection, the input features included time series data of precipitation, maximum temperature, and minimum temperature obtained from multiple gridded climate data products namely ERA5-Land, CHIRPS, MERRA-2, CPC UPP, NASA POWER, and CFS. These datasets were compared against observed station data from the Pakistan Meteorological Department to assess their representativeness. For GCM evaluation, the input features consisted of bias-corrected daily precipitation and temperature values derived from ten CMIP6 models under SSP2-4.5 and SSP5-8.5 pathways. The XGBoost model used these variables to compute feature importance scores, identifying the most reliable datasets and GCMs for climate analysis in District Swat.

Shapley Additive explanations (SHAP):

The interpretation of machine learning models is noteworthy because it helps to better select and understand liable input variables influencing the output decisions. Shapley Additive exPlanations (SHAP) were proposed by Lundberg and Lee (2017) and combines game theory with the purpose of explaining the impact of each feature on the result of the model. SHAP gives each feature a number in which it contributes to how far the prediction is away from being average. This process provides two types of explanations of model behavior: the overall (global) and the individual (local). SHAP values go further and average the effect of a feature across all possible combinations of the inputs, giving a balanced and fair perspective of feature importance [11].

Online Data Source Selection:

The feature importance scores are actual numbers useful in the process of choosing the most pertinent features for the model. Higher scores signify greater importance, meaning the feature has a larger impact on the model's predictions. These scores may be used in the process of determining or choosing the appropriate online data sources to analyze to ensure that whatever data is collected shows a formidable nexus with the observed data. In the current

work stream, the XGBoost model was applied to calculate the feature importance scores on online data sources [12].

In this study, the XGBoost algorithm was implemented to determine the relative importance of different climate data sources and global climate models (GCMs) based on their ability to replicate observed climatic conditions in District Swat. For the evaluation of online data sources, the input features included daily time series data for precipitation, maximum temperature, and minimum temperature obtained from six gridded datasets: ERA5-Land, CHIRPS, MERRA-2, CPC Unified, NASA POWER, and CFSv2. These were compared against the observed station data from the Pakistan Meteorological Department. Similarly, for GCM selection, input features comprised downscaled and bias-corrected daily precipitation and temperature data from ten CMIP6 models under both SSP2-4.5 and SSP5-8.5 scenarios. The model computed feature importance scores using decision tree-based ranking, enabling the identification of the most representative datasets and models for climate analysis in the study region.

GCM Models Selection:

One of the methods of correcting the data is referred to as bias correction. It is usually applicable in improving the outcomes of GCMs (Global Climate Models). GCMs are computerized programs that use mathematical rules to replicate the functioning of the atmosphere, ocean, and land. While these models attempt to predict Earth's climate, they inherently contain systematic biases. Bias correction adjusts the GCM data to align with real-world observations, enhancing its reliability for decision-making.

Methods of statistical downscaling develop connections between the observed data and the output of GCMs. They are convenient, quicker, and computationally efficient compared to other downscaling approaches. Due to this fact, such methods have frequently been applied by scientists to conduct climatic and hydrological research. In the current project, the **linear scaling method** was used to correct the bias. This method is straightforward and preserves both natural variability and trends in the GCM results.

To support this process, the XGBoost model was applied to calculate feature importance scores for 10 GCMs, allowing the identification of the most suitable models for the region [13].

Mann–Kendall (MK) Trend Test:

Monitoring the trends in climate conditions like temperature and precipitation is essential in climate profiling, especially in the comprehension of long-term effects of global warming and new hydrological patterns. The Mann-Kendall (MK) test has become a widely used statistical tool among the many developed so far, because of its non-parametric characteristic, which makes it appropriate in studying hydro-meteorological time series that tend to have missing/outlier values or even non-normally distributed data. [14][15]. MK test relies on the assumption of monotonicity, which implies that the variable being examined has a monotonic tendency to either increase or decrease over the course of time without specifying whether the tendency is monotonic or not. As a rank-based method, it does not require the data to follow a normal distribution, making it particularly valuable in climate studies where data such as monthly or annual temperature and precipitation often deviate from normality [16].

The Mann-Kendall test has gained wide acceptance in the analysis of long-term trends in climatic variables, particularly in climate risk-prone regions. A typical example is when it is employed in measuring higher temperatures over several decades or even extent of significant fall or rise in rainfall as a result of climatic change. This procedure tends to provide a credible approach to identifying indicators of hydrological change early on in the context of climate profiling, especially in semi-arid and mountainous areas [17]. The MK test is deemed to be best suited where the data is obtained either through weather stations, satellite monitoring, or

climate models that were downscaled. In investigations where Representative Concentration Pathways (RCPs) or Shared Socioeconomic Pathways (SSPs) are used, the MK test can be used to analyze and predict data to inform whether the climate models assume statistically significant trends in the future.

In this study, the Mann–Kendall trend analysis was conducted using meteorological data from a single weather station representing District Swat. As the dataset was point-based and not spatially distributed, spatial interpolation methods such as Inverse Distance Weighting (IDW) or Kriging were not applicable.

Intensity-Duration-Frequency curves (IDF):

One of the well-known methods, the intensity-period-frequency (IDF) relationship, can be viewed as a way to derive the relationship between the rainfall intensity and its duration and the period of recurrence. IDF curves are developed by determining the most appropriate statistical distribution to model the variation of excessive rainfall [18]. The IDF curves play a vital role in hydrologic design and infrastructure planning. An analysis of rainfall frequency plays a role in urban drainage design, flood management, and climate resilience [19]. A record of rainfall generates statistics based on annual maximum rainfall values and will be undertaken through the rainfall record. The annual maximum estimates are used to perform the analysis through the Gumbel distribution and the Gamma distribution to estimate the depth of rainfall of different return periods. The effectiveness of the above distribution methods was determined through Kolmogorov-Smirnov, Anderson-Darling darling and Chi-Squared. The rainfall intensities are then calculated using the depth of rainfall [20]. A three-dimensional relationship is estimated between intensity, duration, and frequency via empirical equations [21]. The relationship between the aforementioned parameters is visualized via IDF curves for different return periods [22].

Results and Discussion:

Online data source:

For both precipitation and temperature, the ERA5 reanalysis dataset exhibited the highest feature importance score among the evaluated online data sources, as demonstrated in Figure 3. Based on its superior performance and consistency with observed patterns, ERA5 was selected as the preferred data source in cases where observed meteorological records were unavailable. This ensured a reliable representation of climatic conditions across the study area, supporting robust analysis in data-scarce regions such as District Swat.

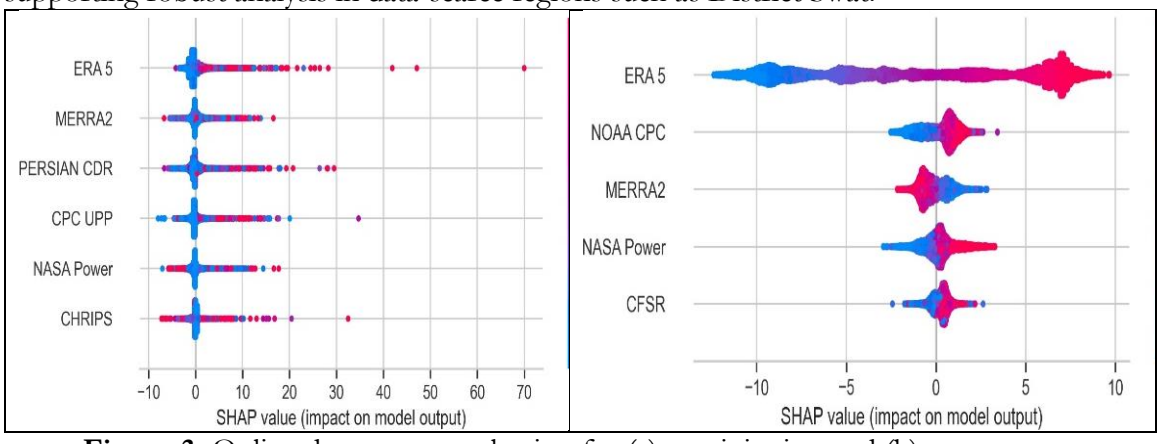

Figure 3. Online data sources selection for (a) precipitation and (b) temperature

GCM Models:

The feature importance score of INM-CM5-0 is the highest, followed by CNRM-CM6-1 (France) and CMCC-ESM2 GCMs, as is obvious from Figure 4. A multi-model ensemble (MME) of the top three models was computed via arithmetic mean.

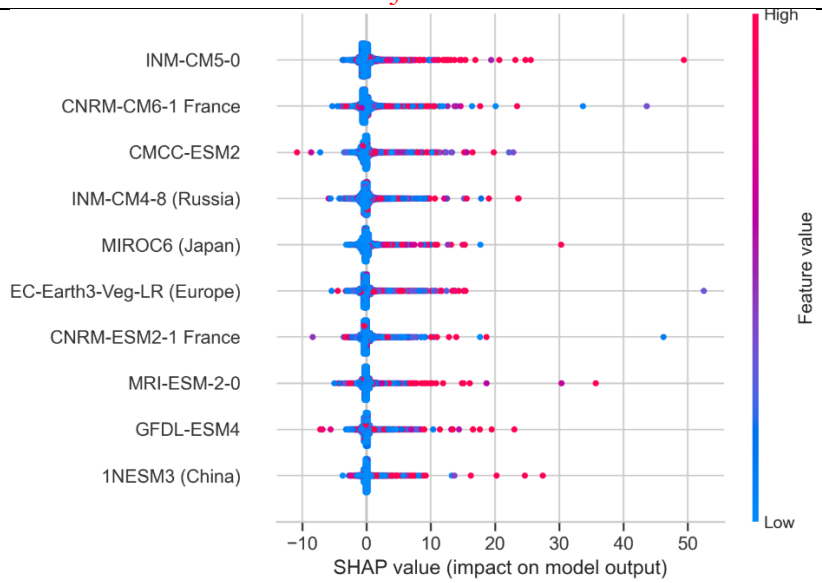

Figure 4. GCM selection

Temperature and Precipitation Regime Over Swat:

The raw observed data, selected top three models, and multi-model ensemble for temperature minimum, temperature maximum, and precipitation are visualized via Parallel Coordinates Plots, as obvious from Figure 5, Figure 6, and Figure 7, respectively. Parallel Coordinates Plots effectively compare multiple GCMs with observed and MME records, which highlight the similarities and differences among the datasets.

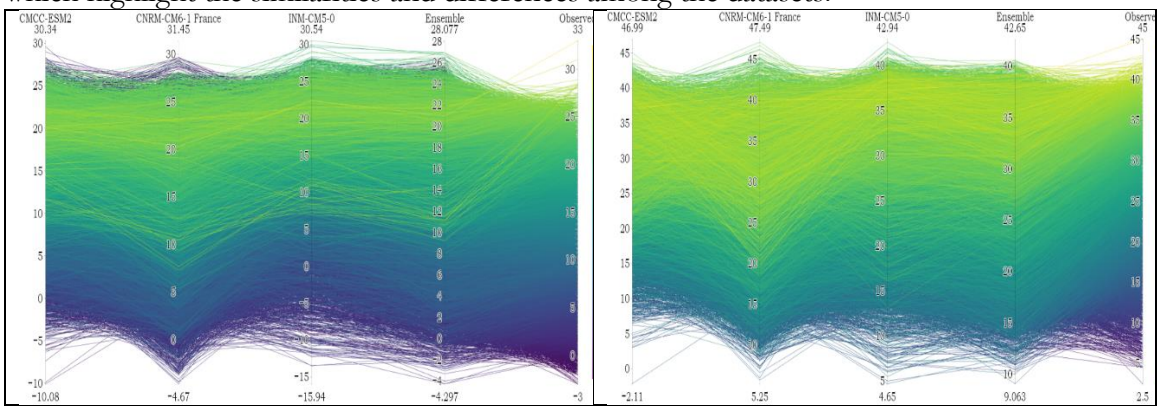

Figure 5. Comparison of the temperature of the selected three models, the observed record, and the MME under SSP245

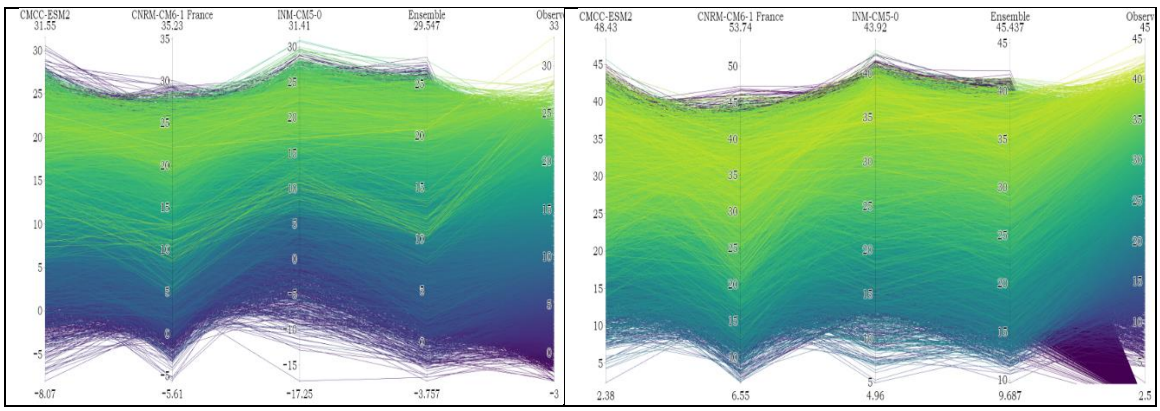

Figure 6. Comparison of the temperature of the selected three models, the observed record, and the MME under SSP585

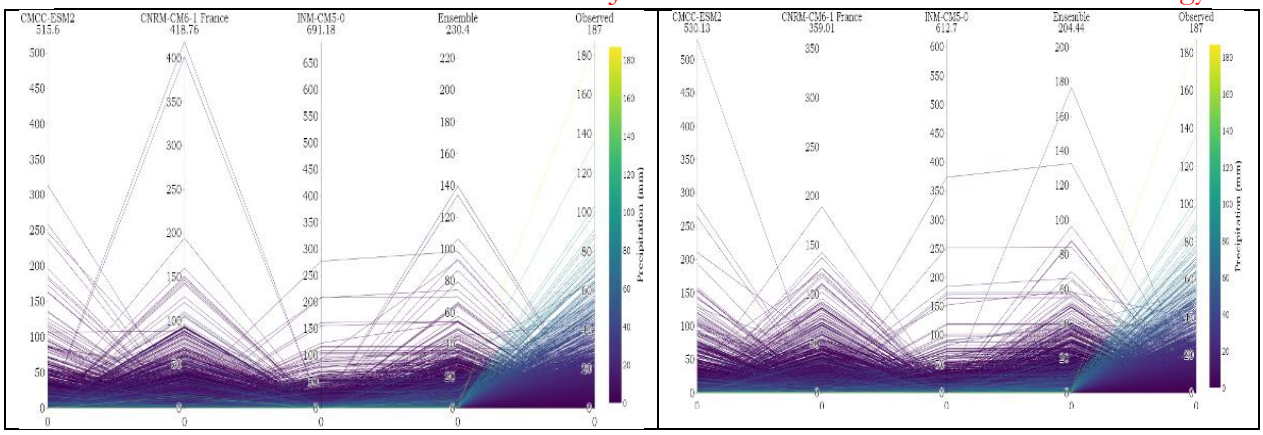

Figure 7. Comparison of precipitation of the selected three models, observed record, and MME under SSP245 and SSP585

Figures 8, 9, and 10 present the variations in minimum temperature, maximum temperature, and precipitation under the SSP2-4.5 and SSP5-8.5 scenarios. The projected temperatures were consistently higher than the observed record under both scenarios. While the overall temporal pattern of precipitation remained comparable between observed and future datasets, the projections, particularly under SSP5-8.5, exhibited occasional extreme precipitation peaks. These anomalies suggest an increased risk of intense rainfall events, which may have critical implications for flood management and agricultural planning in the region.

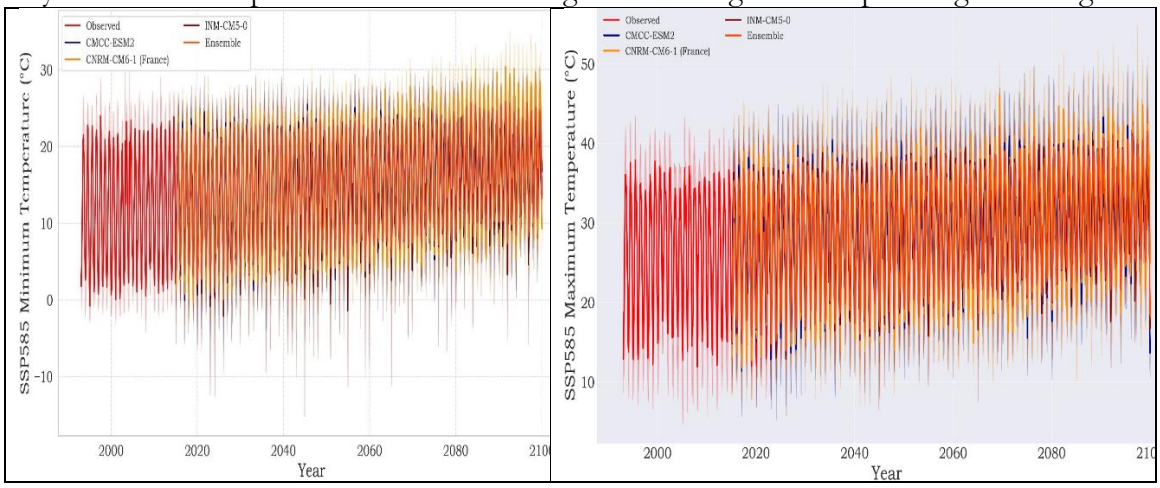

Figure 8. Fluctuations in temperature minimum and maximum under the SSP585 scenario

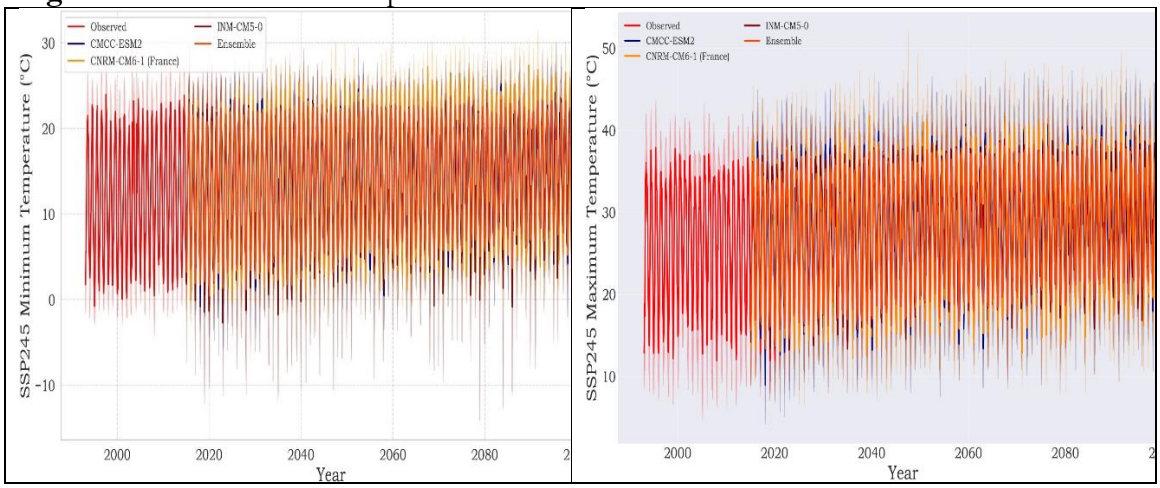

Figure 9. Fluctuations in temperature minimum and maximum under the SSP245 scenario

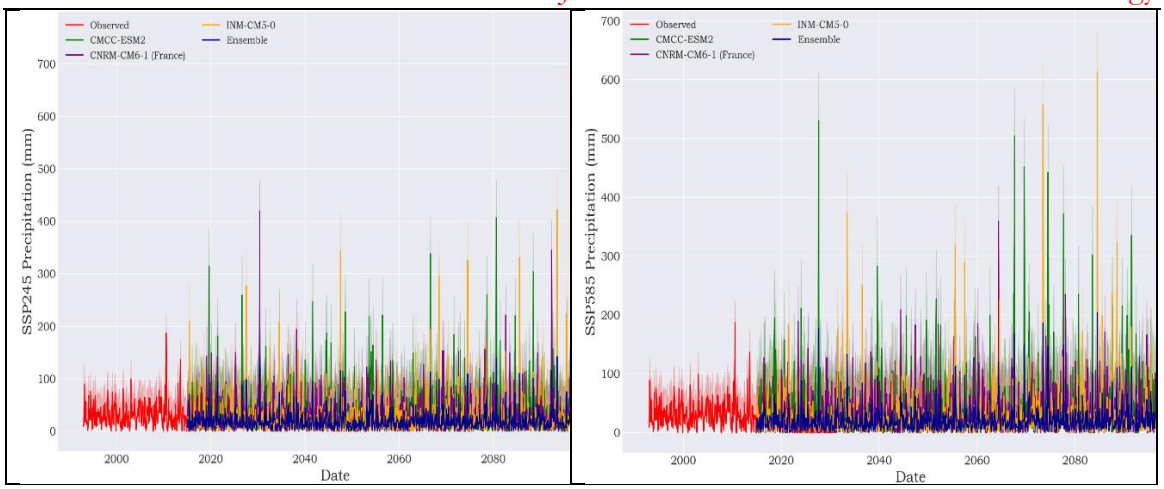

Figure 10. Fluctuations in precipitation under the SSP245 and SSP585 scenarios

Figures 11 and 12 illustrate how daily maximum and minimum temperatures are projected to vary under the SSP2-4.5 and SSP5-8.5 scenarios. These figures compare the observed records with projections for the near future (2015–2042), mid-century (2043–2073), and far future (2074–2099). Over time, the temperature minimum and maximum distribution shifts to the right, indicating a steady increase in nighttime minimum temperatures and daytime maximum temperatures. This suggests that higher minimum and maximum temperatures are likely to occur more frequently in the future. By the end of the century, very cold nights and days almost disappeared, rendering a clear warming pattern that can impact ecosystems, agriculture, and human health. This trend indicates a significant warming pattern for the region, which could have various implications for the local community.

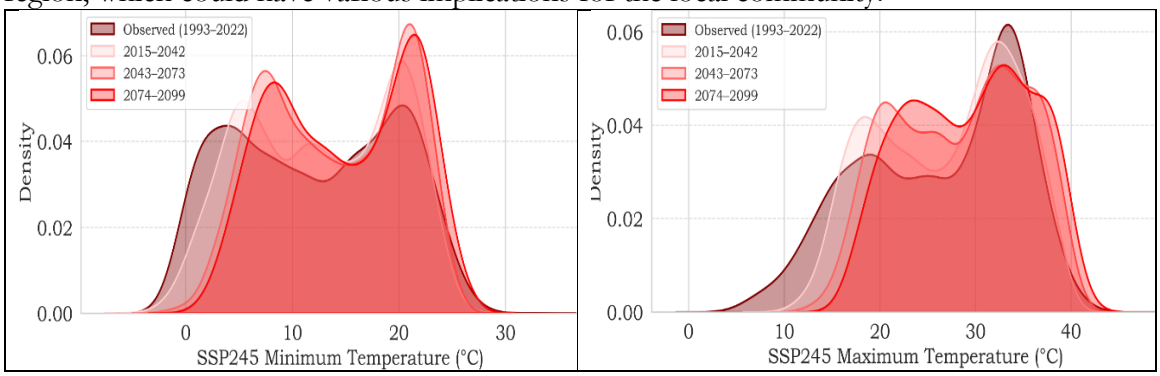

Figure 11. Distribution of T_{min} and T_{max} for various time periods based on SSP245

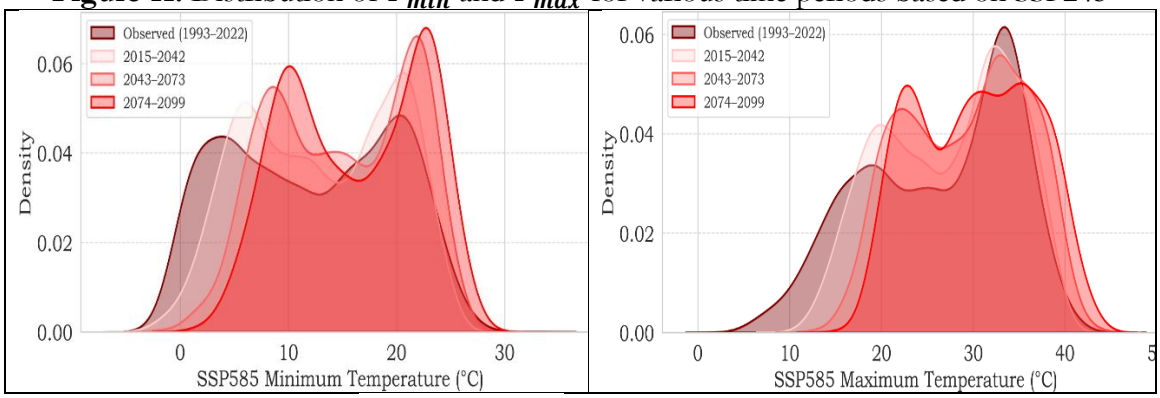

Figure 12. Distribution of T_{min} and T_{max} for various time periods based on the SSP585 scenario

In this study, the reference period was selected from 1993 to 2022. The anomaly in both temperature minimum and maximum under SSP245 ranges between -2 and to 4°C as

demonstrated by Figure 13. Similarly, the anomaly in temperature minimum and maximum under SSP585 ranges between -2 to 6.5°C, and -2 to 6°C respectively, as obvious from Figure 14. The findings of the present study indicate that the temperature anomalies under SSP5-8.5 are greater than those under SSP2-4.5 for both minimum and maximum temperatures. This suggests that District Swat is expected to experience a significantly warmer climate in the future compared to the reference period.

For precipitation, an anomaly was estimated for both SSP scenarios. The anomaly in both SSP245 and SSP585 ranges between -1.5 to 1.5mm and -1.5 to 2mm, as demonstrated by Figure 15. It's worth notable that the anomaly of SSP585 is greater than SSP245. Moreover, both positive and negative anomalies are observed under both SSP scenarios. However, the overall analysis indicates that the Swat District is likely to experience predominantly warmer climate conditions under both SSP2-4.5 and SSP5-8.5 scenarios.

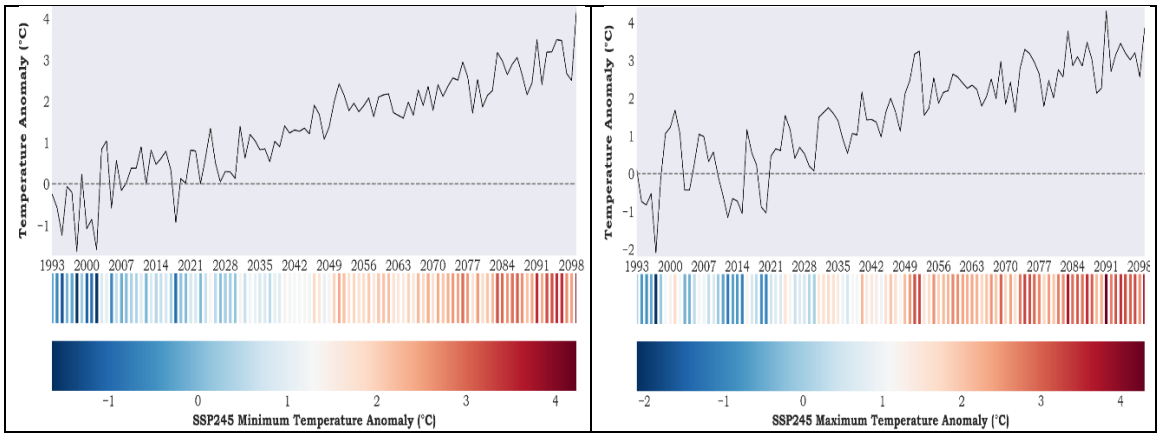

Figure 13. Anomalies in minimum and maximum temperatures under the SSP245 scenario

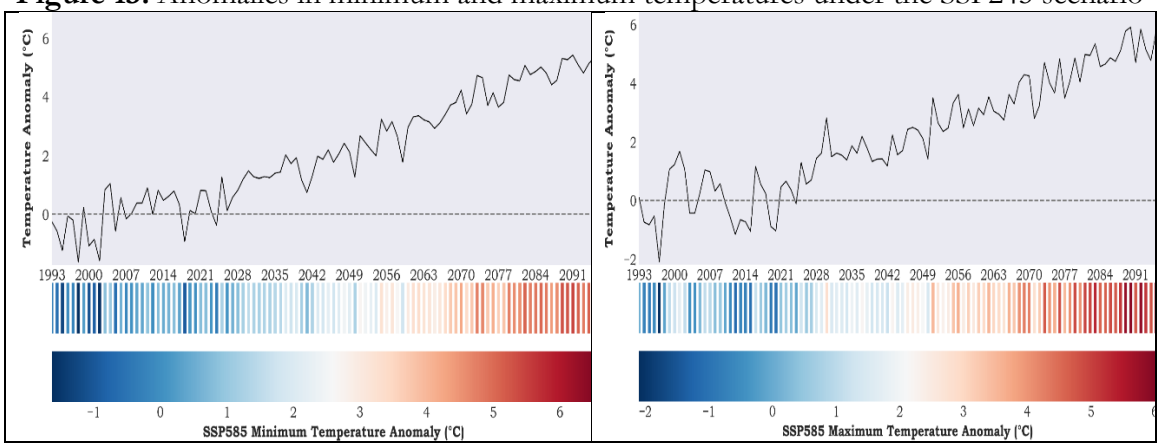

Figure 14. Anomalies in minimum and maximum temperatures under the SSP585 scenario

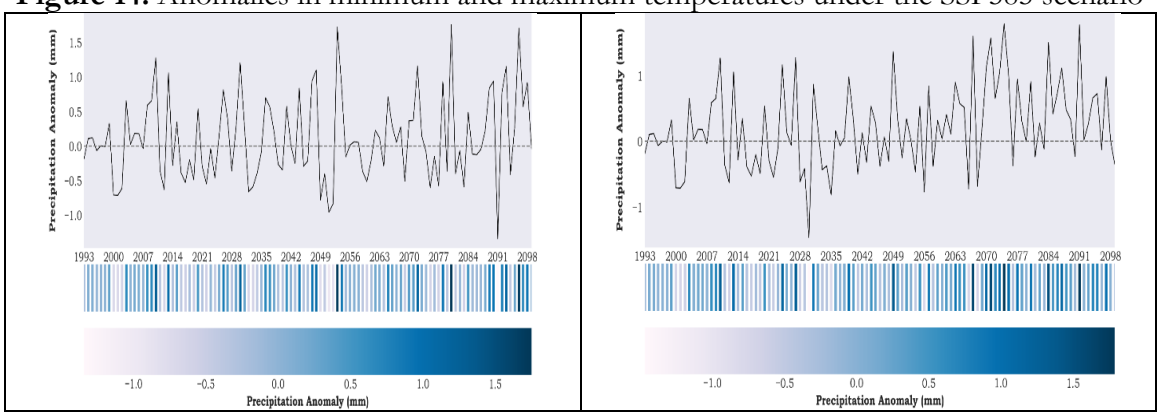

Figure 15. Anomaly in precipitation under (a) SSP245 and (b) SSP585 scenarios

Trend analysis:

Table 1 reveals significant increasing trends in both minimum and maximum temperatures under the SSP2-4.5 and SSP5-8.5 scenarios. In contrast, the trend in observed maximum temperature was not statistically significant. It is noteworthy that future temperature projections exhibit an increasing trend, indicating that temperatures in the Swat District are expected to rise in the coming years. SSP245 exhibited a statistically significant decreasing trend. The observed precipitation and SSP585 trends were not statistically significant. These findings suggest that the project area is likely to experience a hotter and drier climate in the future. Based on this projection, climatologists, hydrologists, and policymakers can formulate informed adaptation strategies to effectively manage the challenges associated with a warming and drying environment.

Table 1. Trend analysis of meteorological parameters for Swat

Variable	Scenario	P value	Tau	Sen's slope	Trend
Tmax	Observed	$9.69E^{-01}$	-0.000246778	0	not significant
	SSP 245	$1.18E^{-91}$	0.076873984	$9.17E^{-05}$	significant
	SSP 585	0	0.151741629	0.000181726	significant
Tmin	Observed	$2.98E^{-09}$	0.037989938	$1.31E^{-04}$	significant
	SSP 245	$5.17E^{-115}$	0.086276308	$9.38E^{-05}$	significant
	SSP 585	0	0.170008459	0.000187718	significant
Precipitation	Observed	0.52229641	-0.004685319	0	not significant
	SSP 245	0.013469954	-0.010281459	0	Significant
	SSP 585	0.378404411	0.003656326	0	not significant

Frequency Analysis of Precipitation:

The IDF curve shows the three-dimensional relationship between rainfall duration, intensity, and return period. Longer return period (100-year) corresponds to higher rainfall intensities, while shorter return period (2-year) corresponds to lower intensities, as is obvious from Figure 16. The observed data, SSP245 and SSP585, curve peaks at the 100-year return period with the highest rainfall intensity of 340mm/hr, 345mm/hr, and 360mm/hr, respectively, and suggest that extreme rainfall events are more intense. Notably, the rainfall intensities of SSP scenarios were greater than the observed record, as is obvious from above. The observed, SSP245, and SSP585 data reflected traditional IDF curve behavior, where intensity decreases with shorter return periods and vice versa. To determine the most suitable statistical distribution for modeling extreme rainfall events in the study area, three commonly used distributions, Gumbel**,** Gamma, and Log-Normal, were evaluated. The performance of each distribution was assessed using multiple goodness-of-fit tests, including the Kolmogorov-Smirnov (K-S) test, the Anderson-Darling (A-D) test, and the Chi-Square test. Among the tested distributions, the Gumbel distribution consistently yielded the lowest K-S and A-D statistics**,** indicating a better fit to the annual maximum rainfall data. Based on these results, the Gumbel distribution was selected for constructing Intensity–Duration–Frequency (IDF) curves for both observed and projected climate scenarios. The rainfall intensities of SSPs were higher than observed records, rendering the importance of climate-resilient infrastructure design to withstand the rare but severe rainfall events.

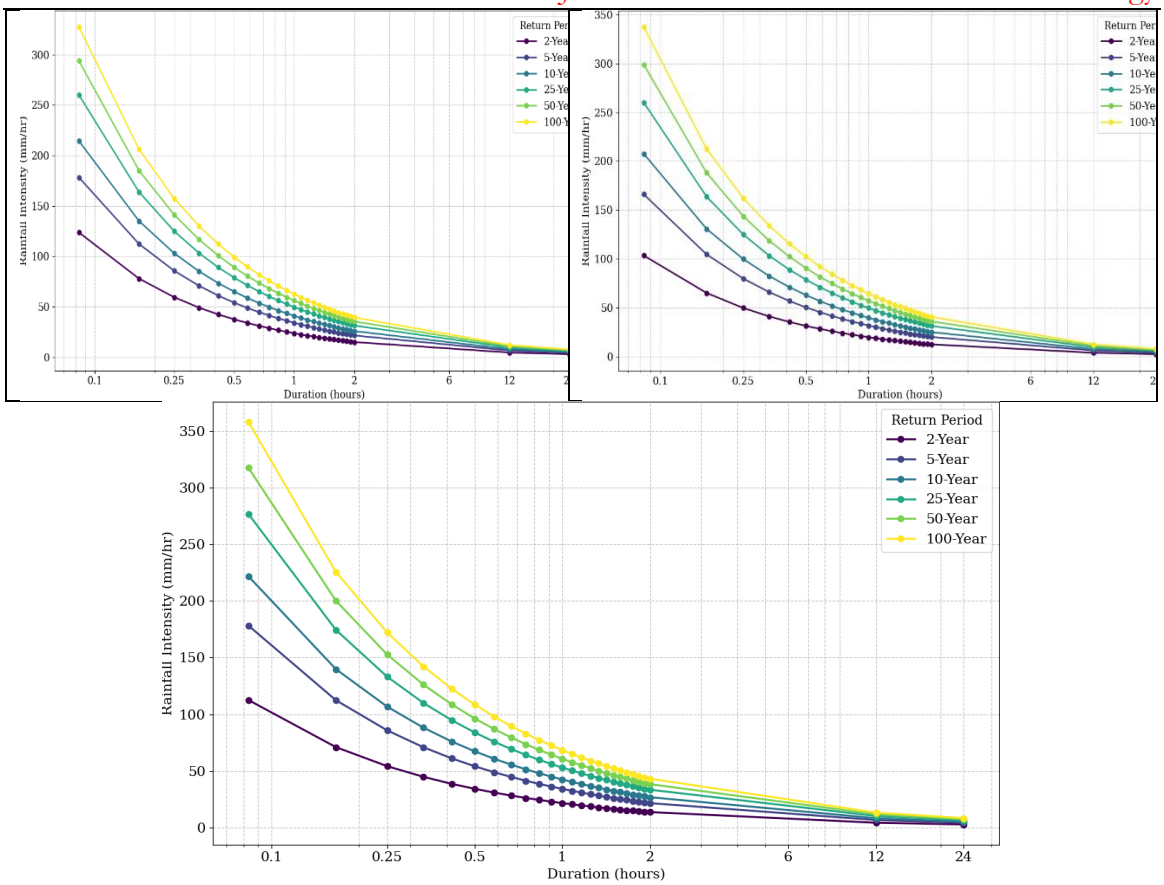

Figure 16. IDF curve for (a) observed conditions, and future conditions under (b) SSP245 and (c) SSP585 scenarios

Discussion:

This study indicates a significant warming trend in the District Swat across SSP2-4.5 and SSP5-8.5. Maximum and minimum temperatures were shown to increase significantly, especially in SSP5-8.5, where Tau was recorded to be 0.1517. These trends are consistent with global projections that indicate a rise in surface temperatures towards the end of the century.[23]. The maximum temperature anomaly of +6.5 °C under SSP5-8.5 points to the possibility of a threat to the existence of snow and glacier-based hydrological regimes in mountains. This warming may accelerate glacier melt rates, change the timing of runoffs, and change the seasonal ablation of water in the area [24]. The above analysis also revealed that precipitation reduced considerably under the SSP2-4.5, which represented a drying tendency in the area. This is consistent with the predictions made on South Asia, where precipitation will become less predictable in the middle emission scenarios and more variable [23]. Nonetheless, based on the intensity-duration-frequency (IDF) analysis, it is projected that the rainfall extremes in the future would become stronger. For instance, the 100-year return period rainfall is estimated to increase by 20mm/hr or 340mm/hr to 360mm/hr under SSP5-8.5, which implies a higher risk of flash flooding and exceedance of the infrastructure capacity. These data align with the observed and simulated trends, indicating an increase in the intensity of extreme rainfall events associated with global warming, even over relatively short observation periods. There is also similar rainfall intensification in monsoon-dominated areas of South Asia, such as northern Pakistan, where the warming has caused an increased frequency of storm events, but decreased concentration of rainfall falling within those events [25]. The application of model selection (XGBoost and SHAP) based on machine learning algorithms ensured transparency and resilience in the selection of the most appropriate GCMs

and online data sets. Using explainable AI in assessing climate models improves the confidence of regional climate projections [26]. This study demonstrates that the District Swat is extremely susceptible to future hydro-climatic change. Rising temperatures, severe precipitation events, a rise in seasonal variability, and more stressful weather conditions raise the necessity to plan resilience to climate change, early warning systems, and sustainable management to meet such arising challenges.

Conclusion:

The climate profile of the district of Swat indicates the massive conversion of the physical environment due to climate change. Projections have shown that the future weather will continue to get warmer in all seasons, with winter becoming milder and summers getting warmer. These results are reassured by observational results and downscaled climate model data. These changes would influence the water needs of crops, increase glacier break-up, and have consequences on the health of the people and the productivity of livestock in the area. Take an in-depth look at the climate changes to conclude that indeed there is a change of climate with Swat expected to heat up under SSP2-4.5 and SSP5-8.5, and get drier, especially in the case of SSP2-4.5. These changes will strain the current storage systems of water and alter future agricultural schedules, hence the need to create climate-fortified water systems.

The evidence of air warming, changes in the precipitation regime, and shifts in intensity–duration–frequency (IDF) curves all point to increasing climatic instability in the region. Such changes will have a considerable impact on food output, water safety, the feasibility of infrastructure, and disaster response. Hence, there is a vital need to develop and put in place an adaptive strategy that would be resilient to climate change in the agriculture, public health, and infrastructure and water management sectors as a way of achieving long-term environmental as well as socio-economic sustainability.

References:

[1] "Prediction of Discharge Using Artificial Neural Network and IHACRES Models Due to Climate Change," *J. Renew. Energy Environ.*, vol. 8, no. 3, pp. 75–85, 2021, Accessed: Jul. 28, 2025. [Online]. Available: https://www.magiran.com/paper/2305515/prediction-of-discharge-using-artificial-neural-network-and-ihacres-models-due-to-climate-change?lang=en

[2] A. B. S. & M. F. P. B. Walter W. Immerzeel, L. P. H. van Beek, M. Konz, "Hydrological response to climate change in a glacierized catchment in the Himalayas," *Clim. Change*, vol. 110, pp. 721–736, 2012, [Online]. Available: https://link.springer.com/article/10.1007/s10584-011-0143-4

[3] P. Friedlingstein *et al.*, "Update on CO2 emissions," *Nat. Geosci.*, vol. 3, no. 12, pp. 811–812, Dec. 2010, doi: 10.1038/NGEO1022;SUBJMETA=106,169,172,704,824;KWRD=ATMOSPHERIC+CHEMISTRY,CLIMATE+SCIENCES.

[4] J. P. Eylon Shamir, Sharon B. Megdal, Carlos Carrillo, Christopher L. Castro, Hsin-I Chang, Karletta Chief, Frank E. Corkhill, Susanna Eden, Konstantine P. Georgakakos a, Keith M. Nelson, "Erratum to 'Climate change and water resources management in the Upper Santa Cruz River, Arizona' [J. Hydrol. 521 (2015) 18–33]," *J. Hydrol.*, vol. 257, p. 1190, 2015, doi: https://doi.org/10.1016/j.jhydrol.2015.04.067.

[5] G. K.-B. Tamiru Paulos Orkodjo, "Impact of climate change on future precipitation amounts, seasonal distribution, and streamflow in the Omo-Gibe basin, Ethiopia," *Heliyon*, vol. 8, no. 6, p. e09711, 2022, [Online]. Available: https://www.cell.com/heliyon/fulltext/S2405-8440(22)00999-9?_returnURL=https%3A%2F%2Flinkinghub.elsevier.com%2Fretrieve%2Fpii%2FS2405844022009999%3Fshowall%3Dtrue

[6] A. H. Md. Rabiul Islam, Md. Tareq Aziz, H. M. Imran, "HEC-HMS-based future

streamflow simulation in the Dhaka River Basin under CMIP6 climatologic projections," *Res. Sq.*, 2024, [Online]. Available: https://www.researchsquare.com/article/rs-4519681/v1

[7] F. G. Matilde García-Valdecasas Ojeda, Fabio Di Sante, Erika Coppola, Adriano Fantini, Rita Nogherotto, Francesca Raffaele, "Climate change impact on flood hazard over Italy," *J. Hydrol.*, vol. 615, p. 128628, 2022, doi: https://doi.org/10.1016/j.jhydrol.2022.128628.

[8] H. W. Muhammad Adnan, Baohua Xiao, Shaheen Bibi, Peiwen Xiao, Peng Zhao, "Addressing current climate issues in Pakistan: An opportunity for a sustainable future," *Environ. Challenges*, vol. 15, p. 100887, 2024, doi: https://doi.org/10.1016/j.envc.2024.100887.

[9] M. S. Islam Bahadar, "Flood hazard assessment using hydro-dynamic model and GIS/RS tools: A case study of Babuzai-Kabal tehsil Swat Basin, Pakistan," *J. Himal. Earth Sci.*, vol. 48, no. 2, p. 7, 2015, [Online]. Available: http://ojs.uop.edu.pk/jhes/article/view/1953

[10] A. Hawamdeh, A. Tarawneh, Y. Sharrab, and D. Al-Fraihat, "Deep Neural Networks Hydrologic and Hydraulic Modeling in Flood Hazard Analysis," *Water Resour. Manag.*, pp. 1–17, May 2025, doi: 10.1007/S11269-025-04243-1/METRICS.

[11] J.-S. J. Sujith Mangalathu, Seong-Hoon Hwang, "Failure mode and effects analysis of RC members based on machine-learning-based SHapley Additive exPlanations (SHAP) approach," *Eng. Struct.*, vol. 219, p. 110927, 2020, doi: https://doi.org/10.1016/j.engstruct.2020.110927.

[12] M. K. A. U. K. S. K. F. A. Khan, "Assessing the impacts of climate change on streamflow dynamics: A machine learning perspective," *Water Sci Technol*, vol. 88, no. 9, pp. 2309–2331, 2023, doi: https://doi.org/10.2166/wst.2023.340.

[13] S. L. Xiaoguang Yuan, "Feature Importance Ranking of Random Forest-Based End-to-End Learning Algorithm," *Remote Sens.*, vol. 15, no. 1, p. 5203, 2023, doi: https://doi.org/10.3390/rs15215203.

[14] G. C. Sheng Yue, Paul Pilon, "Power of the Mann–Kendall and Spearman's rho tests for detecting monotonic trends in hydrological series," *J. Hydrol.*, vol. 259, no. 1–4, pp. 254–271, 2002, doi: https://doi.org/10.1016/S0022-1694(01)00594-7.

[15] K. H. Hamed and A. R. Rao, "A modified Mann-Kendall trend test for autocorrelated data," *J. Hydrol.*, vol. 204, no. 1–4, pp. 182–196, 1998, doi: https://doi.org/10.1016/S0022-1694(97)00125-X.

[16] K. Kendall, "Thin-film peeling-the elastic term," *J. Phys. D. Appl. Phys.*, vol. 8, no. 13, p. 1449, Sep. 1975, doi: 10.1088/0022-3727/8/13/005.

[17] R. Sneyers, "Climate Chaotic Instability: Statistical Determination and Theoretical Background," *Environmetrics*, vol. 8, no. 5, pp. 517–532, Sep. 1997, doi: 10.1002/(SICI)1099-095X(199709/10)8:5<517::AID-ENV267>3.0.CO;2-L.

[18] H. O. S. Dawit T. Ghebreyesus, "Development and Assessment of High-Resolution Radar-Based Precipitation Intensity-Duration-Curve (IDF) Curves for the State of Texas," *Remote Sens*, vol. 13, no. 15, p. 2890, 2021, doi: https://doi.org/10.3390/rs13152890.

[19] J. Chen and B. J. Adams, "Development of analytical models for estimation of urban stormwater runoff," *J. Hydrol.*, vol. 336, no. 3–4, pp. 458–469, 2007, doi: https://doi.org/10.1016/j.jhydrol.2007.01.023.

[20] M. I. K. F. A. K. A. U. K. B. U. A. A. J. G. A. M. A.-A. A. T. B. Taha, "Future precipitation patterns: investigating the IDF curve shifts under CMIP6 pathways," *J. Hydroinformatics*, vol. 27, no. 3, pp. 357–380, 2025, doi: https://doi.org/10.2166/hydro.2025.092.

[21] D. Koutsoyiannis, D. Kozonis, and A. Manetas, "A mathematical framework for studying rainfall intensity-duration-frequency relationships," *J. Hydrol.*, vol. 206, no. 1–2, pp. 118–135, 1998, doi: https://doi.org/10.1016/S0022-1694(98)00097-3.

[22] G. T. Alain Mailhot, Sophie Duchesne, Daniel Caya, "Assessment of future change in intensity–duration–frequency (IDF) curves for Southern Quebec using the Canadian Regional Climate Model (CRCM)," *J. Hydrol.*, vol. 347, no. 1–2, pp. 197–210, 2007, doi: https://doi.org/10.1016/j.jhydrol.2007.09.019.

[23] IPCC, "Climate Change 2007: The Physical Science Basis — IPCC." Accessed: Aug. 11, 2022. [Online]. Available: https://www.ipcc.ch/report/ar4/wg1/

[24] K. M. S. Julia Regnery, Jonghyun Lee, Zachary W. Drumheller, Jörg E. Drewes, Tissa H. Illangasekare, Peter K. Kitanidis, John E. McCray, "Trace organic chemical attenuation during managed aquifer recharge: Insights from a variably saturated 2D tank experiment," *J. Hydrol.*, vol. 548, pp. 641–651, 2017, doi: https://doi.org/10.1016/j.jhydrol.2017.03.038.

[25] F. E. L. Otto *et al.*, "Climate change increased extreme monsoon rainfall, flooding highly vulnerable communities in Pakistan," *Environ. Res. Clim.*, vol. 2, no. 2, p. 025001, Mar. 2023, doi: 10.1088/2752-5295/ACBFD5.

[26] M. Reichstein *et al.*, "Deep learning and process understanding for data-driven Earth system science," *Nat. 2019 5667743*, vol. 566, no. 7743, pp. 195–204, Feb. 2019, doi: 10.1038/s41586-019-0912-1.